Schweizerische Eidgenossenschaft
Confédération suisse
Confederazione Svizzera
Confederaziun svizra

Eidgenössisches Departement für
Umwelt, Verkehr, Energie und Kommunikation UVEK

Bundesamt für Energie BFE

MATERIALS DEVELOPMENT FOR SOLAR THERMOELECTRIC GENERATORS

SOLAR-TEP

Jahresbericht 2007

Autor und Koautoren	Rosa Robert and Anke Weidenkaff
beauftragte Institution	Empa
Adresse	Überlandstrasse 129
Telefon, E-mail, Internetadresse	+41 44 823 41 31, anke.weidenkaff@empa.ch
BFE Projekt-/Vertrag-Nummer	101706 / 152070
BFE-Projektleiter	Anke Weidenkaff
Dauer des Projekts (von – bis)	2006-2008
Datum	19.11.2007

ZUSAMMENFASSUNG

Cobaltate phases are suitable materials for thermoelectric applications at high temperature. Complex cobalt oxide phases are synthesized by “Chimie douce” and classical methods. These potential thermoelectric materials are characterized with respect to their crystal structure, microstructure, composition, and thermal stability by EXAFS, XRPD, EM/ED, TGA, XRF, HGE and DSC.

The Seebeck coefficient, thermal conductivity and electrical resistivity of polycrystalline cobaltates with perovskite-type and layered-cobaltite structure are evaluated in a wide temperature range. The electrical transport of epitaxial La(Co,Ni)O_3 thin films grown by pulsed laser deposition are compared with its bulk counterpart.

The perovskite structure possesses a very high degree of compositional flexibility being able to tolerate a wide variety of cations on both the *A*- and *B*-site and allowing the fine tuning of physical properties. In this experimental study, the influence of *B*-site substitution in the $LaCoO_3$ system is reported. In the studied *B*-site substituted $LaCoO_3$ phases, the charge carrier concentration plays an important role in the enhancement of the electrical transport. The comparison of the electrical transport of La(Co,Ni)O_3 thin films with the polycrystalline phase reveals that the thin films display better thermoelectric performance at high temperatures.

The large Seebeck coefficient exhibited by both perovskite-type and layered cobaltite phases is analysed using the Heikes formula. It can be concluded that the thermopower in cobaltate phases is governed by the spin and orbital degeneracy of the electronic states of the Co ions.

Projektziele

A large amount of the energy we use today comes from limited and non-renewable resources such as fossil fuels. The use of this energy releases polluting emissions into the atmosphere which generate unpredictable influences on our environment. Additionally, they draw on finite resources. In contrast, renewable energy resources like hydrogen, wind and solar energy are constantly replenished. Over the last twenty years there have been major steps accomplished in the development of renewable energy technologies such as wind turbines, photovoltaic (solar cells) systems, thermoelectric devices [1-5], for both industrial and domestic use. However, intensive research is still needed to improve the efficiency in the implementation of "green" energy sources like solar power [6].

Currently, the utilization of Thermoelectric Generators (TEG) for the use of renewable energies and for the recovery of waste heat appears as resurgent technology.

The scope of thermoelectric applications depends on the thermoelectric energy conversion efficiency by means of the temperature difference over which the device is operating and the so called thermoelectric Figure of merit *Z*. *Z* is defined as $Z = S^2/\rho\kappa$, where *S* is the Seebeck coefficient or thermopower, ρ is the electrical resistivity, and κ is the thermal conductivity (S^2/ρ is known as the Power Factor PF). The optimization of the Figure of merit is still a challenge to be solved taking into account that *S*, ρ, and κ are interdependent. Recent thermoelectric research is focused on searching materials with large *S*, low ρ, and low κ in order to realize an efficient conversion of thermal energy into electrical energy. "Classic" thermoelectric materials such as bismuth tellurides and Si-Ge alloys display good thermoelectric properties (ZT ~ 1.2). However, their practical application to power generation in the temperature range of 600 K < T < 1000 K is limited due to problems such as low melting- decomposition-, oxidation or temperature stability, and high toxicity.

The Solar-TEP project is based on the idea of the potential use of concentrated solar heat [7-9] as energy source for Solar Thermoelectric Generators (Solar-TEG). This motivation is directly linked to the development of novel functional materials with enhanced Figures of merit, high temperature stability (T ≥ 400 K), and without harmful elements.

Oxide ceramics show prospective use at high temperatures due to their chemical stability against thermal oxidation in air. Consequently, thermoelectric modules based on oxide materials have the advantage to enlarge the operating range of temperature and thus, the generated output power. Additionally, thermoelectric oxide devices can be realised on the basis of low cost materials with low toxicity. All these facts lead to the selection of transition metal oxides as focus of this study.

Furthermore, we also study epitaxial thin film thermoelectrics [10, 11]. A number of low dimension structures such as nano-structured materials, thin films, and superlattices have been proposed to improve the thermoelectric properties of materials. In particular, thin films should exhibit a decreased of the thermal conductivity due to an increased phonon scattering, while an increased local electron density of states may improve the thermopower [12].

Durchgeführte Arbeiten und erreichte Ergebnisse

1. Thermopower of the $LaCo_{1-x}Ni_xO_3$ series and the Heikes equation:

The thermopower measurements of the polycrystalline $LaCo_{1-x}Ni_xO_3$ samples ($0.0 \leq x \leq 0.30$) [13], in the temperature range of $300\ K \leq T \leq 1240\ K$ and also at $T \leq 300\ K$ for x = 0.02, are presented in Figure 1. The Seebeck coefficient is positive indicating predominant positive mobile charge carriers for all the Ni-substituted compositions. The substitution of Co by Ni in the $LaCo_{1-x}Ni_xO_3$ system increases the carrier concentration, as shown in the resistivity data, leading to a reduction of the absolute Seebeck coefficient value at room temperature. In the temperature range of 250 K < T < 300 K, the *S* varies only weakly with temperature. In the low substitution range where the conduction is generated by a hopping mechanism, the temperature-independent thermoelectric power can be described by Heikes formula [14]:

$$S = +\frac{k_B}{|e|} ln\left(\frac{1-c_h}{c_h}\right) \qquad \textbf{(Eq. 1)}$$

where k_B is the Boltzmann's constant and c_h is the fraction of Co site occupied by a positive charge carrier. Applying this formula to e.g. x = 0.02, the theoretical Seebeck coefficient reaches a value of S ~ + 350 µV/K, which is in good agreement with the experimental value of $S_{exp(300K)}$ = + 360 µV/K. For x

= 0.10, the theoretical Seebeck coefficient adopts a value of S ~ + 200 µV/K which corresponds to $S_{exp(300K)}$ = + 173 µV/K at room temperature. In the inset of Figure 1, the room temperature values of *S* for $LaCo_{1-x}Ni_xO_3$ (scatters) are plotted as a function of nickel content x and the solid line describes the theoretical values derived from Heikes equation. The experimental room temperature data for the low substitution range, x ≤ 0.15, are well described by Heikes formalism. However, the $LaCo_{1-x}Ni_xO_3$ becomes metallic for a higher Ni content and thus, the experimental Seebeck coefficient does not follow this theoretical approach.

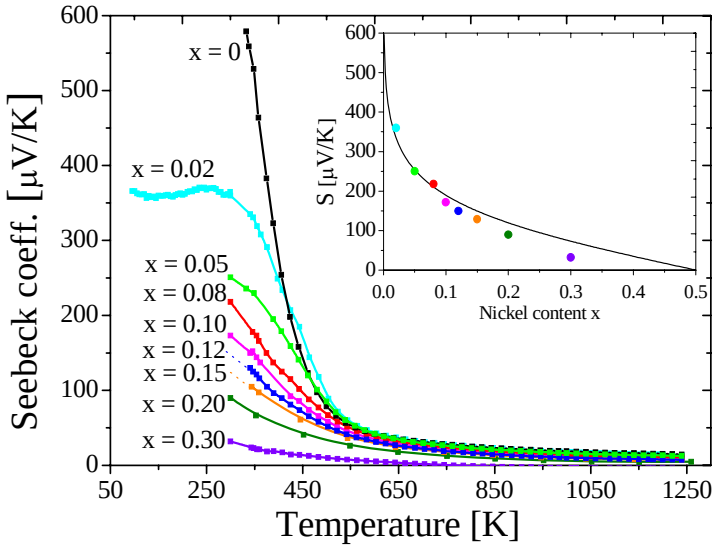

Figure 1: Thermopower of $LaCo_{1-x}Ni_xO_3$ ($0.0 \leq x \leq 0.30$) as a function of temperature in the temperature range of 300 K ≤ T ≤ 1240 K and also at T ≤ 300 K for x = 0.02; room temperature *S* data (scatters) and Heikes equation fit (solid line).

2. PLD $LaCo_{0.92}Ni_{0.08}O_3$ thin films

Epitaxial thin films grown on inactive substrate materials offer a suitable alternative to large single crystals as "two-dimensional" crystal and the possibility to study the influence of the dimensionality on the thermoelectric properties. $LaCo_{0.92}Ni_{0.08}O_3$ thin films are grown on MgO substrates by Pulsed Laser Deposition (PLD) technique. Thin films are characterized concerning crystallinity, morphology and composition. The transport properties are compared with the parent polycrystalline phase.

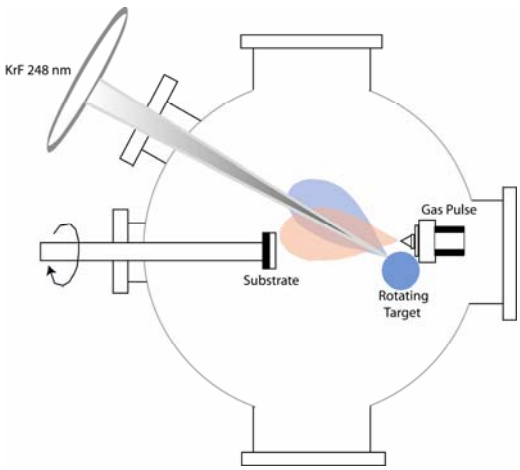

Figure 2: Scheme of the pulsed reactive crossed-beam laser ablation (PRCLA) setup. A synchronized reactive gas pulse interacts close to the target with the ablation plumes. The plasma species are deposited on a rotated heated substrate.

$LaCo_{0.92}Ni_{0.08}CoO_3$ thin films of different thickness (~ 86 nm, ~220 nm, and ~ 395 nm) were grown on MgO (100) substrates by Pulsed Reactive Crossed-beam Laser Ablation (PRCLA), (see Figure 2). PRCLA is a variation of PLD. In PRCLA, the ablation process is supplemented by a reactive gas which may affect the ablation plume species in the gas phase [15-17]. The $LaCo_{0.92}Ni_{0.08}CoO_3$ films were

deposited using a KrF excimer laser (λ = 248 nm, 20 ns pulse width and variable number of pulses) with a laser fluence of 3.0 J/cm2 and a repetition rate of 10 Hz. The target material was produced from the pressed and sintered $LaCo_{0.92}Ni_{0.08}CoO_3$ powders prepared by soft chemistry method as described in [10].

Structure, crystalline quality and texture of the films have been studied with a Siemens D5000 X-ray diffractometer with Bragg–Brentano geometry using Cu K_α radiation. The (θ- 2θ) scan performed on $LaCo_{0.92}Ni_{0.08}O_3$ films grown in MgO substrate revealed the formation of the crystalline perovskite phase. XRD patterns of the films with thicknesses of ~220 nm and ~ 395 nm show the presence of La_2O_3 phase. On the contrary, the LCNO film with a thickness of ~ 90 nm (LCNO-I in the following) does not contain reflections arising from secondary phases. Figure 3a presents a (θ- 2θ) scan for the LCNO-I at χ = 0°. The LCNO thin films crystallize in the rhombohedral crystal structure with $R\bar{3}c$ S.G., having lattice parameters of ≈ $a_p\sqrt{2}$ x $a_p\sqrt{2}$ x 2 $a_p\sqrt{3}$, γ = 120° in hexagonal settings, as reported in [18] for the parent $LaCo_{0.92}Ni_{0.08}O_3$ polycrystalline compound.

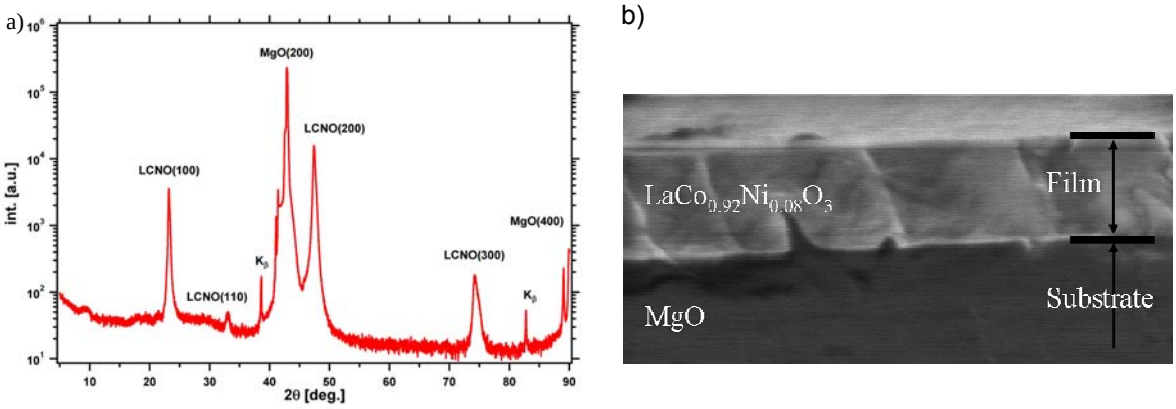

Figure 3: a) XRD pattern and b) cross-sectional SEM-view of the LCNO-I film grown on MgO.

Figure 3b shows the cross section SEM image of the LCNO-I thin film. The film with light contrast corresponds to the $LaCo_{0.92}Ni_{0.08}O_3$ thin film and the substrate with dark contrast corresponds to the MgO (100). The film thickness measured by a profilometer is around 86 nm with a roughness in the range of 6.9 nm and 8.1 nm. The film thickness obtain from RBS data has a value of 108 nm.

The elemental composition was analyzed by Rutherford backscattering experiments (RBS) at the Department of Ion Beam Physics ETHZ. RBS results reveal that the composition of the LCNO-I film is $La_{1.06 \pm 0.03}(Co, Ni)_{1.00}O_{2.96 \pm 0.09}$. The LCNO-I film has the same composition as the starting target material. Thus, RBS and PIXE results confirm a congruent ablation of the $LaCo_{0.92}Ni_{0.08}O_3$ phase.

Electric transport measurements have been used to characterize physical properties of the LCNO-I film. Figure 4 shows the thermopower and the electrical resistivity of the LCNO-I thin film and LCNO polycrystalline sample.

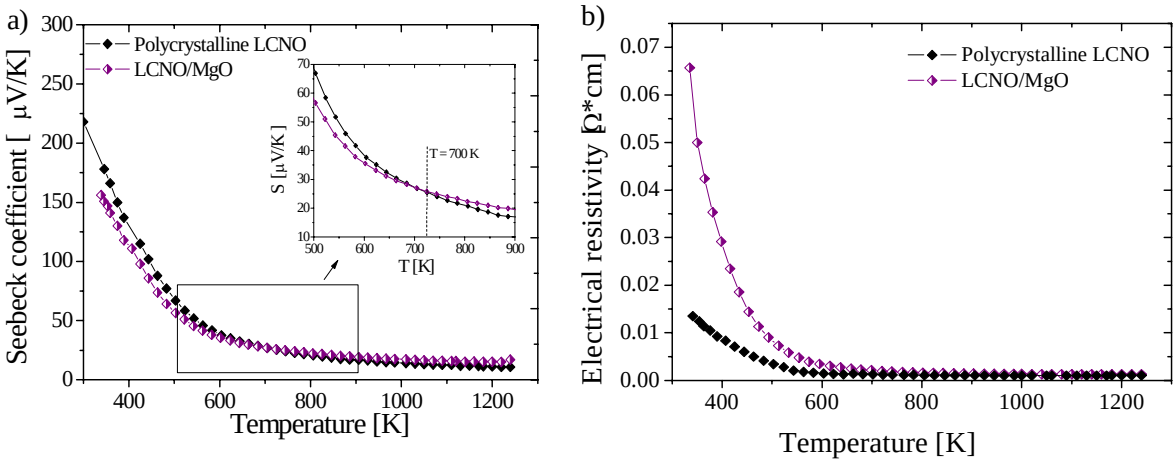

Figure 4: a)Thermopower and b) electrical resistivity of the polycrystalline- and thin film La-$Co_{0.92}Ni_{0.08}O_3$ phase as a function of temperature in the temperature range of 350 K ≤ T ≤ 1240 K.

The thin film exhibits a higher value of electrical resistivity and a comparable value of the thermoelectric power with respect to the polycrystalline sample at room temperature. These results show that the dimension of the material has an effect on the electrical resistivity but not on the Seebeck coefficient.

The ρ(T)-curves for both materials present a similar behaviour in the whole measured temperature range. However, the *S*(T)-curves present a crossing at T = 700 K. As a result, the thin film shows higher thermoelectric performance at high temperatures.

3. The misfit cobaltite "$Ca_3Co_4O_9$"

The misfit cobaltite phases with the composition $Ca_{3-x}Ba_xCo_4O_9$ (0.0 ≤ x ≤0.02) and $Ca_3Co_{3.80}B_{0.20}O_9$ (with B = Fe and Ti) were obtained by thermal decomposition of the corresponding amorphous citrate precursor [7].

The thermal stability of the misfit phases was evaluated by thermogravimetric analysis using a Netzsch STA 409 CD thermobalance. The experiments were carried out under oxidizing (O_2: He = 20:80) atmosphere with a gas flow rate of 50 ml/min. The samples were heated up to T = 1150 K with a heating rate of 10 K/min, and further cooled down with the same heating rate. DSC/ TG measurements of $[Ca_2CoO_3][CoO_2]_{1.62}$, shown in Figure 6, reveal four thermal events.

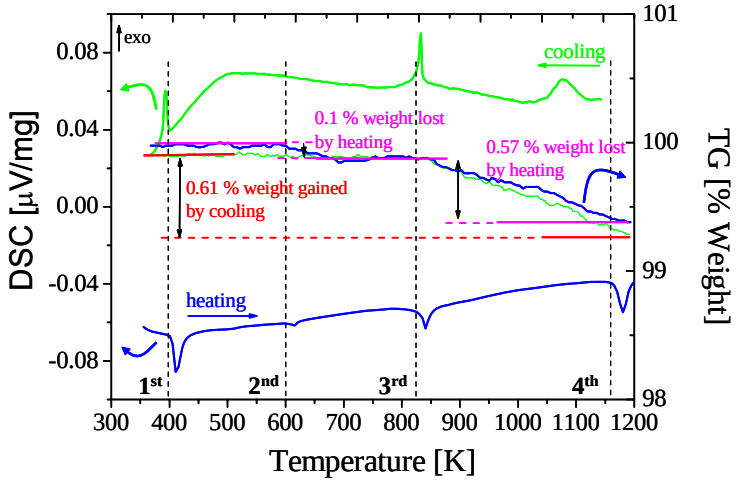

Figure 6: DSC/ TG measurements plot versus temperature for the $[Ca_2CoO_3][CoO_2]_{1.62}$ compound.

The DSC/ TG experimental data reveal that the oxygen content in the misfit cobaltite changes with temperature: i) an increase in temperature leads to oxygen losses, i.e. thermal reduction and ii) the

oxygen loss is reversible and with decreasing temperature the misfit compound restores its original oxygen content, i.e. re-oxidize.

The changes in the oxygen stoichiometry will have an immediate effect on its electrical resistivity, as it will be explained later.

The crystal structure of the misfit cobaltite has an important effect on the transport properties observed in this system. As is shown in Figure 7, the Co ions in the [CoO_2] layers show a trigonal symmetry. Consequently, the electronic states of the Co ions in an octahedral field, i.e. t_{2g} and e_g orbitals, further degenerate into the non-degenerated a_{1g} and the twofold degenerated e'_g orbitals. Large density of states at the Fermi level (E_F) found in the narrow a_{1g} band are responsible for the large Seebeck coefficient, while charge carriers in the e'_g band are responsible for the metallic conductivity [19].

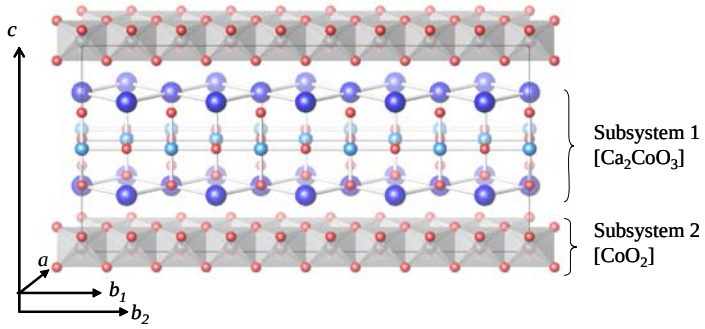

Figure 7: Structural model of the $[Ca_2CoO_3][CoO_2]_{1.62}$ misfit cobaltite.

The Seebeck coefficient values for all the misfit cobaltites are positive indicating *p*-type conduction. The thermopower of the misfit phase is relatively large (S = + 120 μV/K) at room temperature despite of the metallic behaviour. All the studied phases present a similar Seebeck coefficient value in the range of + 119 μV/K ≤ S ≤ 121.3 μV/K at T = 330 K, independently from the atomic substitution.

In layered cobalt oxides, Co ions are found in a trigonal lattice where the 3*d* electrons are strongly degenerated due to spin and orbital degrees of freedom. The formal valence of Co ions is between + 3 and + 4. The thermopower in these oxides can be fitted by:

$$S = +\frac{k_B}{|e|} ln\left(\frac{g_4}{g_3}\frac{1-c_h}{c_h}\right) \qquad \textbf{(Eq. 2)}$$

which considers that the dominating contribution to the thermopower is the entropy of the degenerated charge carriers. c_h denotes the content of Co^{4+} ions and g_3 (g_4) is the number of possible configurations of the Co^{3+} (Co^{4+}) ions, [20].

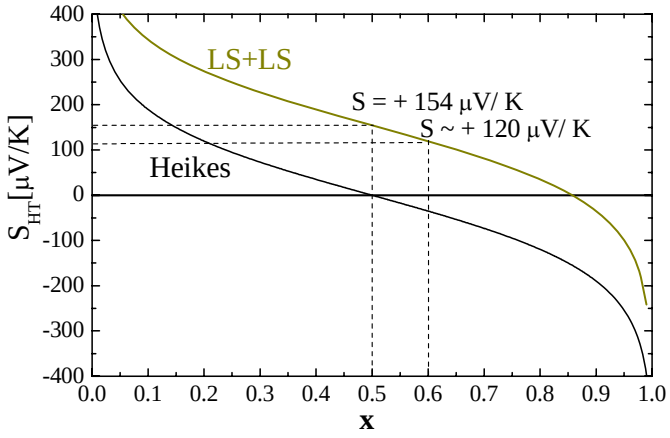

Figure 7: Thermopower calculated for cobaltates considering (1) Heikes equation (Eq. 1) and (2) Eq 2 with g_3/g_4 = 1/6 as a function of the charge carrier concentration x (c_h).

The estimated high temperature thermopower by Eq. 2 is S = + 154 µV/K, assuming a value of the Co valence of + 3.5 and taking into account the low spin state of Co^{3+} (t_{2g}^6) and low spin state of Co^{4+} (t_{2g}^5) in the CoO_6 layer. The ratio g_3/g_4 = 1/6 implies a low-spin configuration of Co^{3+} and Co^{4+} ions. This approximation also holds the suggestion that the low-spin states of Co^{3+} ions are responsible for the large thermopower found in these systems. Based on Eq. 2, the thermopower values of S ~ + 120 µV/K at T = 300 K for all the studied misfit cobaltites result in an estimated value of the Co valency of $u_{Co} \approx 3.6$, considering that $u_{Co} = c_h + 3$, where c_h is the concentration of holes and equal to 0.6.

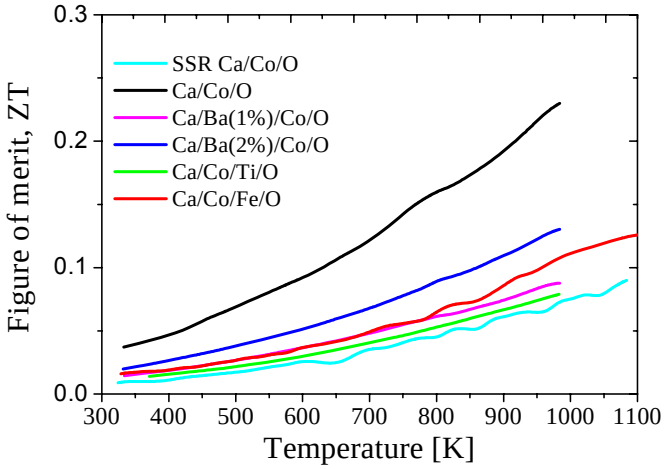

Figure 8: Figure of merit for the misfit phases in the temperature range of 340 K ≤ T ≤ 1100K.

Figure 8 shows the temperature dependence of the Figure of merit, $ZT = \frac{S^2}{\kappa\rho}T$, in the tempera

ture range of 340 K ≤ T ≤ 1100 K. For all the samples, the *ZT* increases with increasing temperature. The misfit cobaltite compound prepared by soft chemistry route exhibits the highest *ZT* values over the measured temperature range and reaches a value of ZT = 0.23 at T = 985 K, which is in good agreement with reported *ZT* values of polycrystalline sample at high temperature, e.g ZT ~ 0.22 at T = 1000 K for spark plasma sintered $Ca_3Co_4O_9$ [21].

4. Summary and conclusions

Summarising the results, it can be stated that the thermoelectric properties of the complex cobalt oxides are influenced by many parameters as synthesis procedure, oxidation state and spin-state of the cobalt ion, oxygen stoichiometry. The soft chemistry approach is an appropriate alternative to prepared pure cobalt oxide phases.

In the $LaCo_{1-x}Ni_xO_3$, the decrease of the electrical resistivity, observed when the Ni content increases, can be attributed to the increase of Co^{4+} ions and thus, to the number of holes in the mixed ($Co^{3+/4+}$) valence band. The temperature dependence of the electrical resistivity follows ($\rho(T) \sim exp(E_a/kT)$), as expected for a thermally activated process. The activation energy E_a decreases with increasing Ni content. The electrical resistivity values of polycrystalline pressed pellets are similar to the reported values for single crystals. These results lead to the conclusion that the grain boundaries and pores do not hinder the electrical transport. The thermopower of these phases is positive indicating that the electronic transport is made by holes-like carriers. Large *S* is preserved for low level substitution in good accordance with the Heikes equation.

The single crystalline $LaCo_{0.92}Ni_{0.08}O_3$ thin film exhibits a higher value of the electrical resistivity and similar value of the thermoelectric power compared with the polycrystalline sample. These results show that the Seebeck coefficient is not sensitive to the sample dimensions. On the contrary, the electrical transport may be affected by the strain in the film-substrate interface. The thin films display better thermoelectric performance at high temperatures.

The thermoelectric properties displayed by the misfit cobaltites i.e. a large Seebeck coefficient, poor thermal conduction together with a metal-like good electrical conduction demonstrate the large potential of these oxides for high temperature applications.

Nationale Zusammenarbeit

- Thin films growth by Pulsed laser deposition, S. Heiroth and Dr. Th. Lippert, Paul Scherrer Institut.
- Ion Beam Physics, Dr. Max Döbeli, Paul Scherrer Institut and ETH Zürich.
- Neutron diffraction (ND) and X-ray diffraction (XRD) experiments at SINQ and SLS

Internationale Zusammenarbeit

- X-ray diffraction (XRD) and X-ray absorption spectroscopy (XAS) experiments at HASYLAB/DESY, Hamburg.
- Half- hausler compounds, Prof. Dr. Claudia Felser, Uni Mainz.
- Prof. Dr. Armin Reller, Uni Augsburg is the doctor father of the PhD candidate.

Bewertung 2007 und Ausblick 2007+1

A future work related to the present study will be to perform in-situ high temperature neutron diffraction studies. These experiments can yield information about structure on different length scales, phase and chemical composition, dynamic phase formation, phase decomposition and phase transition processes which can influence the materials behaviour at the operational temperature in the application.

Referenzen

[1.] M. A. Green, ***Solar Energy Conversion*** in **Materials for energy conversion devices**. Editors: Ch. C. Sorrel S S, J. Nowotny. Woodhead Publishing Limited, Abington Hall, Abington. Cambridge: England, 2005.

[2.] I. Terasaki, ***Introduction to thermoelectricity*** in **Materials for energy conversion devices,** Editors: Ch. C. Sorrel S S, J. Nowotny,., Woodhead Publishing Limited, Abington Hall, Abington: Cambridge: England, 2005.

[3.] W. Shin, N. Murayama, K. Ikeda, and S. Sago, ***Thermoelectric power generation using Li-doped NiO and (Ba, Sr)PbO_3 module***, aus J. Power Sources, 103, Seiten 80-85, 2001.

[4.] R. Funahashi, M. Mikami, T. Mihara, S. Urata, and N. Ando, ***A portable thrmoelectric-power-generating module composed of oxide devices***, aus J. App. Phys., 99, Seiten 066117, 2006.

[5.] E. S. Reddy, J. G. Noudem, S. Hebert, and C. Goupil, ***Fabrication and properties of four-leg oxide thermoelectric modules***, aus J. Phys. D: Appl. Phys., 38, Seiten 3751-3755, 2005.

[6.] Aldo Steinfeld, ***Solar thermochemical production of hydrogen - a review***, aus Solar Energy, 78, Seiten 603-615, 2005.

[7.] R. Robert, S. Romer, A. Reller, and A. Weidenkaff, ***Nanostructured complex cobalt oxides as potential materials for solar thermoelectric power generators***, aus Adv. Eng. Mater., 7, Seiten 303-308, 2005.

[8.] R. Robert, L. Bocher, M. Trottmann, A. Reller, and A. Weidenkaff, ***Synthesis and high-temperature thermoelectric properties of Ni and Ti substituted $LaCoO_3$***, aus J. Solid State Chem., 179, Seiten 3867–3873, 2006.

[9.] R. Robert and A. Weidenkaff, ***SOLAR-TEP***, aus BfE-Abschlussbericht, 2006.

[10.] R. Robert, M. H. Aguirre, L. Bocher, M. Trottmann, S. Heiroth, T. Lippert, M. Döbeli, and A. Weidenkaff, ***Thermoelectric properties of polycrystalline samples and epitaxial $LaCo_{1-x}Ni_xO_3$ thin films***, submitted to Solid State Sciences, 2007.

[11.] M. H. Aguirre, S. Canulescu, R. Robert, N. Homazava, D. Logvinovich, L. Bocher, T. Lippert, and A. Weidenkaff, ***Structure, microstructure and high temperature transport properties of $La_{1-x}Ca_xMnO_{3-d}$; thin films and polycrystalline bulk materials***, accepted in J. Appl.Phys., 2007.

[12.] L. D. Hicks and M. S. Dresselhaus, ***Thermoelectric figure of merit of a one-diemnsional conductor***, aus Phys. Rev. B, 47, Seiten 16631, 1993.

[13.] R. Robert, L. Bocher, B. Sipos, M. Döbeli, and A. Weidenkaff, ***Ni-doped cobaltates as potential materials for high temperature solar thermoelectric converters***, aus Prog. Solid State Chem., 35, Seiten 447-455, 2007.

[14.] R. R. Heikes, R. Mazelsky, and R. C. Miller, ***Magnetic + electrical anomalies in $LaCo0_3$***, aus Physica 30, 8, Seiten 1600-1608, 1964.

[15.] M. J. Montenegro, M. Döbeli, T. Lippert, S. Müller, B. Schnyder, A. Weidenkaff, P. R. Willmott, and A. Wokaun, ***Pulsed laser deposition of $La_{0.6}Ca_{0.4}CoO_3$ (LCCO) films. A promising metal-oxide catalyst for air based batteries***, aus Phys. Chem. Chem. Phys., 4, Seiten 2799-2805, 2002.

[16.] M. J. Montenegro, T. Lippert, S. Müller, A. Weidenkaff, P. R. Willmott, and A. Wokaun, ***Pulsed laser deposition of electrochemically active perovskite films,*** aus Appl. Surf. Sci., 197, Seiten 505-511, 2002.

[17.] M. J. Montenegro, C. Clerc, T. Lippert, S. Müller, P. R. Willmott, A. Weidenkaff, and A. Wokaun, ***Analysis of the plasma produced by pulsed reactive crossed-beam laser ablation of $La_{0.6}Ca_{0.4}CoO_3$***, aus Appl. Surf. Sci., 208, Seiten 45-51, 2003.

[18.] M. H. Aguirre, R. Robert, D. Logvinovich, and A. Weidenkaff, ***Synthesis, crystal structure and microstructure analysis of perovskite type compounds $LnCo_{0.95}Ni_{0.05}O_3$ (Ln = La, Pr, Nd, Sm, Gd and Dy)***, aus Inorg. Chem., 46, Seiten 2744-2750, 2007.

[19.] Y. Miyazaki, ***Crystal structure and thermoelectric properties of the misfit-layered cobalt oxides***, aus Solid State Ionics, 172, Seiten 463-467, 2004.

[20.] W. Koshibae, K. Tsutsui, and S. Maekawa, ***Thermopower in cobalt oxides***, aus Phys. Rev. B, 62, Seiten 6869-6872, 2000.

[21.] D. Wang, L. Chen, Q. Yao, and J. Li, ***High-temperature thermoelectric properties of $Ca_3Co_4O_{9+\delta}$ with Eu substitution***, aus Solid State Commun., 129, Seiten 615-618, 2004.

.